Please do not adjust margins

ARTICLE

Acridinone-based anion transporters†

Daniel A. McNaughton,[a] Lauren K. Macreadie [a] and Philip A. Gale [*a,b]

Received 00th January 20xx,
Accepted 00th January 20xx

DOI: 10.1039/x0xx00000x

The arrangement of hydrogen bond donors around a central lipophilic scaffold has proven a successful strategy in the development of potent chloride transporters. In this work, we revisit an acridinone 1,9-bis(thio)urea motif which had previously shown promise as an anion sensor and expand the series of compounds by appending a variety of electron-withdrawing groups to the peripheral phenyl moieties. High levels of activity were achieved by the most effective compounds in the series, which facilitated strictly electroneutral transport.

Introduction

The discovery of transmembrane anion transporters continues apace[1] driven by the potential application of these compounds in the treatment of diseases such as cancer[2] and cystic fibrosis.[3] A successful strategy to design anionophores is to append hydrogen bond donor groups to a lipophilic scaffold. Examples include cholapods,[4] *ortho*-phenylenes,[5] *trans*-decalins,[6] and anthracenes.[7] We have previously shown that there is an optimal log P for each class of anion transporter.[8,9] Compounds with a low log P value may not be able to efficiently partition into a lipid bilayer whilst compounds with a high log P may not be deliverable and instead need to be pre-incorporated into a lipid bilayer to study their transport properties. We therefore decided to investigate the use of acridinone as a scaffold for a bis-urea and thiourea-based anion transporters. Acridinones are aromatic heterocyclic compounds that exhibit distinct optical properties, resulting from strong absorption and emission in the UV-vis region. These compounds (**1**-**10**) possess a potential additional hydrogen bond donor (as with carbazole bis-ureas)[10] from the acridinone NH group whilst the lipophilicity of the compounds is attenuated by the heteroatoms relative to analogous acridine-based compounds (Figure 1).

We have previously studied acridinones as anion receptors and sensors.[11] Compounds **1** and **6** were found to interact with chloride. Perturbations in the chemical shifts attributed to the (thio)urea protons were fit to a 1:1 receptor:anion binding model and chloride binding constants were determined to be K_a = 273 M^{-1} and K_a = 53 M^{-1} for the bis-urea (**1**) and bis-thiourea (**6**), respectively. In this study we prepared a larger series of bis-ureas and thio-ureas and studied their anion transport properties in phospholipid bilayer membranes.

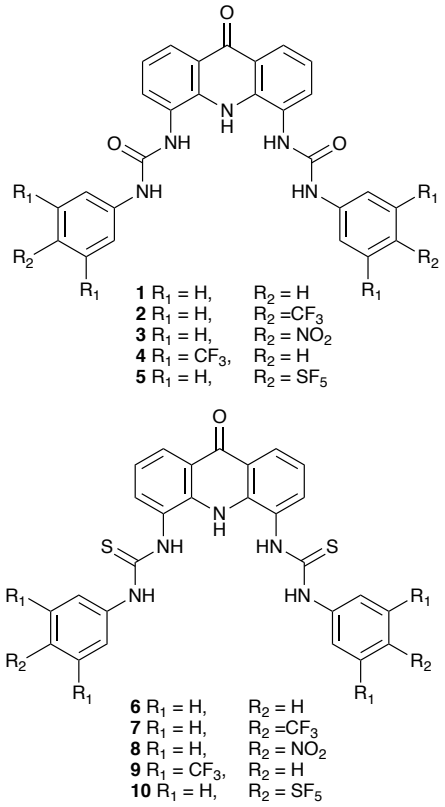

Figure 1 The structures of ureas **1**–**5** and thio-ureas **6**–**10**.

Results and discussion

Synthesis

a. School of Chemistry (F11), The University of Sydney, NSW 2006, Australia.
b. The University of Sydney nano Institute (SydneyNano), The University of Sydney, NSW 2006, Australia.

† Dedicated to friend and colleague Professor Hiroyuki Furuta on the occasion of his 65th Birthday.

Electronic Supplementary Information (ESI) available: synthesis and characterisation details, anion binding and transport studies and X-ray crystallography. See DOI: 10.1039/x0xx00000x

Please do not adjust margins

Please do not adjust margins

The acridinone series was synthesised *via* a four-step synthetic pathway. Initially, 1,9-diaminoacridinone was prepared following the method reported by García-Garrido *et al.*,[11] with alterations made to the method of nitro group reduction. A Jourdan-Ullman condensation reaction between commercially available 2-bromo-3-nitrobenzoic acid and 2-nitroaniline was performed to afford compound **11** (Scheme 1).[12] Copper powder was used as a catalyst in this reaction, which is performed under molten conditions at 190 ℃ for 4 h. The high temperatures required for the reaction are a consequence of the significant deactivation of the bromine position in 2-bromo-3-nitrobenzoic acid. This deactivation was reflected in the poor yields achieved for this step, which did not exceed 30%. Ring closure of the intermediate was initiated by dissolving **11** in conc. H_2SO_4 and heating to 100 ℃ for 1 h to afford the 1,9-dinitroacridinone intermediate **12** in 79% yield.

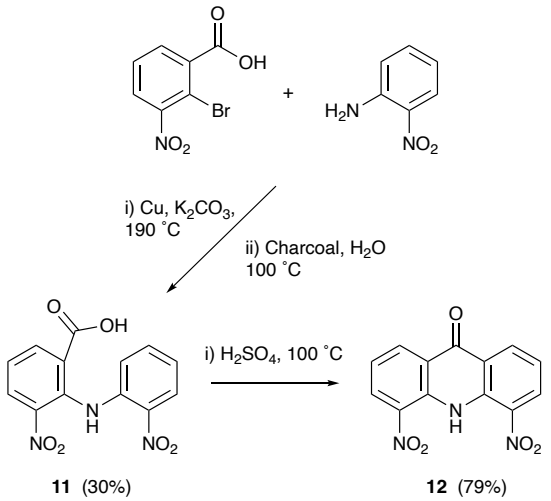

Scheme 1 Synthesis of precursor **12**

Palladium on carbon was used to catalyse the reduction of compound **12** in DMF. The solution was filtered through celite to remove the palladium on carbon, followed by removal of DMF *in vacuo* to afford bis-amine **13** in 94% yield.

The synthesis of compounds **1**–**4** and **6**–**9** was initially attempted by reacting **12** with an excess of the respective isocyanate or isothiocyanate in a minimum amount of dry DMF and the progress was followed by TLC. Upon completion, the reaction mixture was poured into ice water, resulting in precipitation of the desired product and other side products. Residual DMF was removed with additional washes of deionised water and the side products were removed with washes of various non-polar solvent mixtures (see the experimental section for details). DMSO was found to be a suitable alternative solvent and was used in several the iso(thio)cyanate condensation reactions.

4-(Pentafluorosulfanyl)phenyl isocyanate and isothiocyanate and were prepared from 4-pentafluorosulfanylaniline. The isothiocyanate was formed by reacting the aniline with thiophosgene in a biphasic mixture of dichloromethane and sat. $NaHCO_{3(aq)}$ solution, at room temperature. The two phases were separated before the DCM was removed *in vacuo*. The desired 4-(pentafluorosulfanyl)phenyl isothiocyanate product was used without further purification to prevent potential hydrolysation of decomposition and added to a DMSO solution of **13**. Compound **10** was afforded in a 33% yield. To prepare compound **5**, 4-pentafluorosulfanyl aniline and a small excess of triphosgene were dissolved in toluene and heated to 70 ℃.[13] Triethylamine (TEA) was added immediately to neutralise HCl forming in the reaction. After work-up, a solution of **13** in DMF was added dropwise to the solution of 4-(pentafluorosulfanyl)phenylisocyanate in toluene to afford **5** in 63% yield.

X-ray crystallography

Crystals of **3** of suitable quality for analysis using single X-ray crystal diffraction were obtained by slow evaporation of a saturated DMSO solution (CCDC 2101004). Compound **3** crystallises in the space group $P2_1/n$ with one formula unit in the asymmetric unit and two DMSO solvents of crystallisation. Close intramolecular hydrogen bonds cause one of the urea groups to be positioned inwards to the centre of the molecule. This orientation allows for hydrogen bonding between the O3 urea carbonyl acceptor and the acridinone N4 donor group (N4···O3: 2.736(4) Å), and between O3 and the phenyl C5 donor (C5···O3: 2.867 (4) Å). This close hydrogen bonding is also observed for the urea carbonyl O5 (C25···O5: 2.896 (4) Å). Close hydrogen bonds also exist for one DMSO molecule with the outwardly facing urea, forming a R½6 motif between N–H donor groups to the DMSO oxygen acceptor (N2···O8 2.796(4) Å, N3···O8 2.800(4) Å).

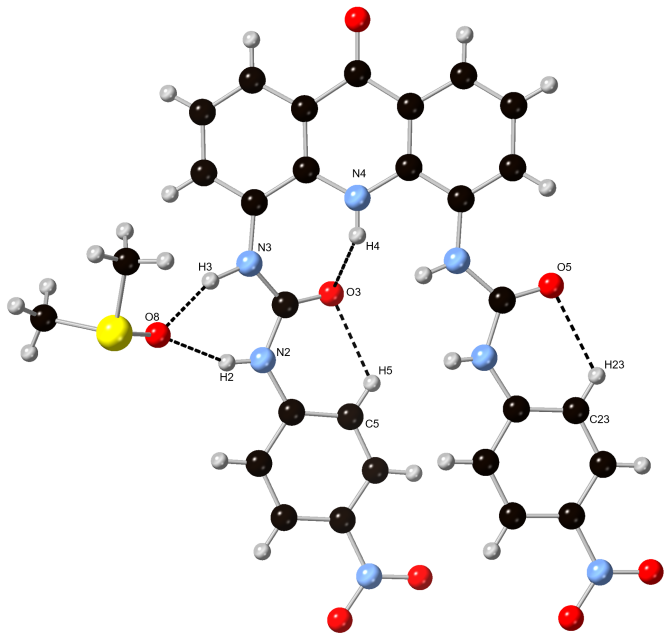

Figure 2 The X-ray crystal structure of the DMSO solvate of receptor **3**.

Please do not adjust margins

Please do not adjust margins

Anion binding studies

Proton NMR titrations were conducted with compounds **1** - **10** in DMSO-d_6/0.5% D_2O and tetrabutylammonium chloride (TBA Cl). Solutions were titrated with up to 300 equivs. of TBACl. Large downfield shifts in the urea or thiourea NH resonances were observed upon addition of TBACl for all the compounds. Interestingly, the resonance attributed to the acridinone N−H proton of bis-urea compounds **1**–**5** responded differently to the addition of TBACl compared to the corresponding resonance in the bis-thiourea compounds **6**–**10**. Stacked plots of the titrations of each compound with TBACl are shown in the supplementary information. For titrations conducted with the bis-urea compounds the acridinone signal initially shifted slightly upfield, before reversing and moving downfield above approx. 10 equiv. of the TBACl. During the Cl^- titrations of the bis-thiourea compounds, the acridinone N−H proton resonance shifted downfield initially before plateauing at higher equivalents.

The change in chemical shift of the resonances for both (thio)urea protons and the acridinone N−H proton upon addition of chloride were fitted to various binding models using the Bindfit applet.[14,15] Fitting to a 1:1 receptor:guest binding model was found to result in a poor fit; however, fitting the data to a 1:2 receptor:guest binding model provided a significant improvement. $Fcov_{fit}$ was calculated for each of the receptors and the covariance of fit of the 1:2 binding model was found to be 8 times greater than the 1:1 binding model for compound **6**, and at least 13 times greater for the other receptors. The reversal in direction of the acridinone N−H proton resonance during titrations of the bis-urea species is additional evidence in support of a higher-order binding model. The fit complementarity suggests that two binding events occur over the course of the titration. The K_{11} and K_{12} binding constants for receptors **1**–**10** are displayed in Table 1.

Table 1 The stability constants (M^{-1}) for the complexation of receptors **1**–**10** and Cl^- (as TBA salt) in DMSO-d_6/0.5% D_2O at 298K.

Compound	K_{11} [a]	K_{12} [a]	α [b]	F cov_{fit} [c]
1	247	- [e]	- [e]	13
2	264	1.3	0.005	90
3	500	2	0.004	158
4	357	3.9	0.01	92
5	328	1.7	0.005	386
6	115	2.4	0.02	8
7	121	2	0.02	53
8	241	3.7	0.02	48
9	183	3.3	0.02	31
10	136	3.3	0.02	22

[a] All errors < 5%. [b] The interaction parameter (α) calculated by multiplying K_{21} by 4 and dividing by K_{11}; a value of α<1 is indicative of negative cooperativity. [c] Factor of covariance of fit ($Fcov_{fit}$) calculated by dividing cov_{fit} 1:2 with cov_{fit} 1:1; a value greater than 5 indicates a 1:2 binding model is favoured.[15] [e] K_{12} value for compound **1** was extremely small.

A potential explanation the contrasting shifts of the acridinone NH proton resonances of the urea and thiourea compounds upon addition of chloride could be the tautomerism of the acridinone group. Previously, we elucidated the solid-state structure of the chloride complex of compound **1** and found it crystallised as the hydroxy tautomer (CCDC 629282).[11] A chloride anion was bound by the protons of the two urea groups, and a second chloride was stabilised by a hydrogen-bonding interaction with the hydroxy O−H donor group.

After examination of the ^{13}C-NMR spectra of compounds **1**−1**0**, the formation of the alternate tautomer could be discounted. Each ^{13}C-NMR spectrum contains a resonance between 176.8−177.4 ppm, which is a fingerprint resonance for the C9 carbon of acridinone in DMSO-d_6. This characteristic resonance is present in numerous acridinone systems reported in the literature,[16,17] including in systems locked in the acridinone form via *N*-substitution.[18-20] In addition, physicochemical studies and theoretical calculations on similar acridinone molecules have confirmed the hydroxyacridine tautomer is not present at equilibrium in DMSO solutions.[16,21,22] A permanent tautomeric switch from the acridinone to the hydroxyacridine form of the system would result in a significant change in the C9 carbon environment, and the ^{13}C-NMR resonance for this carbon in acridine systems is more typically found in the range 140−160 ppm.[23]

Furthermore, the occurrence of tautomerism over the course of the ^{1}H-NMR titrations is unlikely as the signal attributed to the acridinone NH proton resonance remains sharp and can be followed continuously for each titration. However, the appearance of new resonances upon addition of multiple (up to 300) equivalents of chloride during the ^{1}H-NMR titrations of compounds **1**–**5** is evidence in support of tautomerism of the chloride complex that is slow on the NMR timescale. Specifically, the appearance of a new peak at 11.56 ppm in the spectrum of **10** after the addition of 300 equivs. of TBACl (Figure S91) may be attributed to the OH proton of the hydroxyacridine species.

The shift in the bis-urea acridinone NH proton resonance and evidence of a 1:2 receptor:guest binding process can be rationalised by considering that an intramolecular hydrogen bond may form in the free receptor when the urea carbonyl is orientated inwards (Scheme 2a, top structure), akin to the solid-state structure of compound **3** (Figure 2). The same intramolecular hydrogen bond may not be possible in the bis-thiourea compounds **6**–**10** because the bulk of the sulfur atom means the thiourea cannot flip inwards as effectively and sulfur is a poorer hydrogen bond acceptor than oxygen (Scheme 2b). Therefore, the ^{1}H-NMR signal attributed to the acridinone NH proton is shifted further downfield for the bis-urea compounds compared to the bis-thiourea compounds due to deshielding of the proton caused by the intramolecular hydrogen bond.

At low equivalents of TBACl, a 1:1 receptor:guest complex is preferred where the urea carbonyl group flips back to the exterior of the molecule and chloride is bound through N−H hydrogen bonds within the central cavity (Scheme 2a, middle structure). This binding event induces a downfield shift in the signals of the urea protons, which form cooperative hydrogen bonds with chloride, and an upfield shift in the acridinone N−H proton signal due to disruption of the intramolecular hydrogen bond formed with the urea carbonyl oxygen (presumably the

Please do not adjust margins

Please do not adjust margins

hydrogen bond to chloride is less deshielding than the intramolecular interaction with the carbonyl oxygen). At higher host/guest ratios, the equilibrium shifts to a 1:2 receptor:guest complex *via* another conformational switch. This time both urea carbonyl groups flip inwards, and each bind a chloride anion through N−H hydrogen bonds on the exo-face of the complex (Scheme 2a bottom most structure). The acridinone N−H proton resonance begins to shift back downfield due to the reformation of intramolecular hydrogen bonding interactions with the urea carbonyl oxygens. A similar conformational change was proposed for the binding modes of carbazole-based bis-ureas and bis-thioureas.[10]

The thiourea groups of compounds **6**−**10** are initially held closer to perpendicular to the acridinone motif (Scheme 2b, top structure), in a manner similar to the ground state computational studies performed by Dias *et al*. on their anthracene-based thiourea compounds.[7] At lower equivalents of TBACl, a 1:1 receptor:guest complex is preferred with a chloride anion held within the central cavity (Scheme 2b, middle structure). Hydrogen bonding interactions between chloride and all thiourea N−H protons and the acridinone N−H proton cause the ^{1}H-NMR resonances for these protons to collectively shift downfield. At higher equivalents of guest, each thiourea group binds a chloride anion individually as the equilibrium shifts towards a 1:2 receptor:guest complex (Scheme 2b, bottom most structure). The bulky nature of the sulfur atoms means the thiourea groups are oriented perpendicular to the acridinone motif. An intramolecular bonding interaction does not form between the thiourea sulfur atoms and the acridinone N−H proton due to the steric bulk and poorer hydrogen bond acceptor ability of sulfur, and hence the signal attributed to the acridinone N−H proton begins to plateau. The acridinone N−H resonance should in fact move upfield, but the minimal shift experienced by this signal reflects the small amount of 1:2 complex that forms.

The interaction parameter, α (Table 1), was calculated for receptors **1**−**10** and found to be less than 1 in each case,[15] indicating that the 1:1 complex is heavily favoured over the 1:2 complex (negative cooperativity).[24] This, in concurrence with the proposed binding modes presented in Scheme 2, suggests a cooperative binding site featuring multiple hydrogen bonding interactions encapsulating chloride is present in the 1:1 binding complex. The shift to a 1:2 binding complex removes this cooperativity, as reflected in the much smaller K_{12} values compared to K_{11} values for the acridinone series.

An assessment of the K_{11} values suggests that the bis-urea compounds exhibit a higher affinity towards chloride than their bis-thiourea analogues, despite the enhanced acidity of the thiourea protons. The higher binding affinity can be attributed to the planarity in the molecule necessary for optimal binding in the 1:1 complex. The smaller oxygen atoms of the bis-urea receptors are more capable of achieving the required planarity than the bulky thiourea sulfur atoms, which distort the shape of the binding site. A similar phenomenon was observed for bis-(thio)urea based receptors.[7,10]

The trend in K_{11} values for both series of receptors is in agreement with the expected trend when increasingly electron-withdrawing substituents are appended to the peripheral phenyl rings. The parent phenyl receptors **1** and **6** exhibit the lowest affinities for chloride. The K_{11} values for receptors **2** and **7** are smaller than the K_{11} values for **5** and **10**, respectively, highlighting the enhanced electron-withdrawing ability of the *para*-SF_5 group compared to a *para*-CF_3 group. The *para*-NO_2 (**3** and **8**) and 3,5-bis-CF_3 (**4** and **9**) derivatives displayed the highest affinities for chloride, which is consistent with the increased acidity of their (thio)urea protons, induced by the strong electron-withdrawing nature of these substituents.

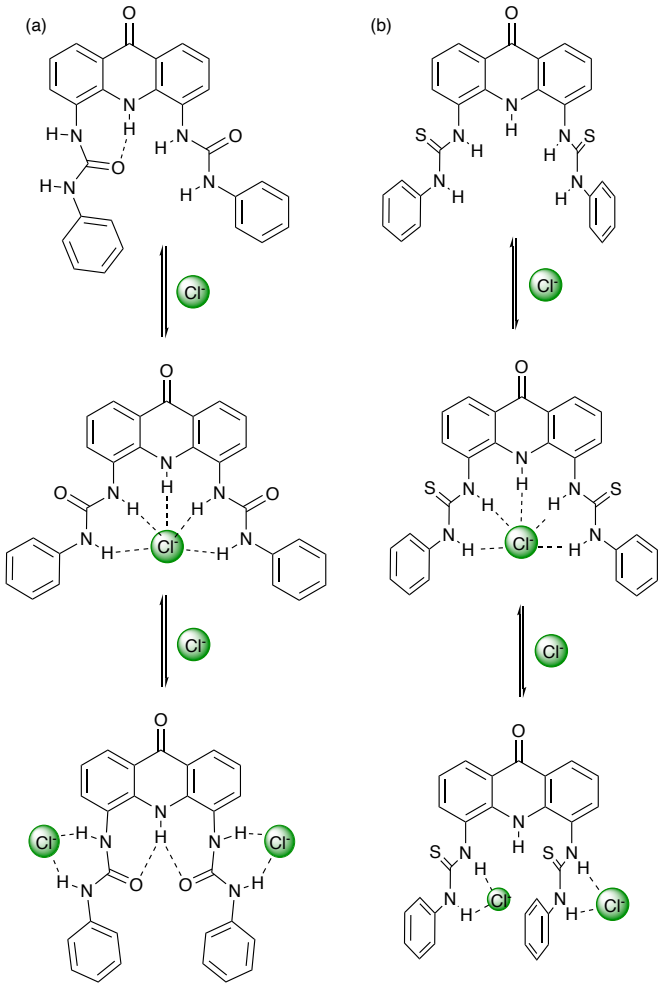

Scheme 2 The general schematic of the proposed binding modes of the bis-urea receptors (a) **1**−**5** and (b) thioureas **6** - **10**. Hydrogen-bonding interactions are depicted as dashed lines.

Anion transport studies

Chloride/nitrate exchange assay

The anion transport activity of acridinone-based bis-(thio)urea receptors **1**−**10** was investigated using the Cl^-/NO_3^- exchange assay (Figure 3).[25] Large unilamellar vesicles (200 nm) were prepared with a NaCl internal solution (487 mM) buffered to pH 7.2 with sodium phosphate salts (5 mM). The vesicles were subsequently suspended in a $NaNO_3$ external solution (487 mM) buffered to pH 7.2 following a similar method. Receptors were

Please do not adjust margins

Please do not adjust margins

added as a DMSO solution (10 µL to a vesicle suspension of 5 mL) at t = 0 s, and chloride efflux was measured using a chloride ion-selective electrode (ISE). Experiments were conducted for 300 s before detergent was added to the vesicles providing the 100% Cl^- efflux reading, which was used for calibration of the results. Dose response studies were performed followed by Hill analysis of Cl^- efflux at 270 s to quantify transport activity.

Dose response studies of compounds **1**, **2**, **6** and **7** could not be completed due to the insolubility of the receptors in aqueous solution at the required concentrations. These compounds proved less active than the other receptors tested, and addition as a DMSO solution at concentrations of 0.5 mol% or higher resulted in precipitation of the receptors. Solubility issues were also found with the *para*-SF_5 receptors **5** and **10**. The receptors both reached a maximum of 75% efflux (270 s) at the highest concentration tested, and convergence in the chloride efflux curves at higher transporter loadings was observed. These findings suggest that receptor **5** reaches its solubility limit at around 0.1 mol%, and **10** at closer to 1 mol%. However, as the final efflux is above 50%, an EC_{50} value could still be reliably calculated for these compounds. The calculated EC_{50} values, which represent the concentration required to facilitate 50% transport, and Hill coefficients, which provide an indication of the stoichiometry required for the transport process, are shown in Table 2. Efflux plots and fitting to the Hill equation for each compound are available in the supplementary information.

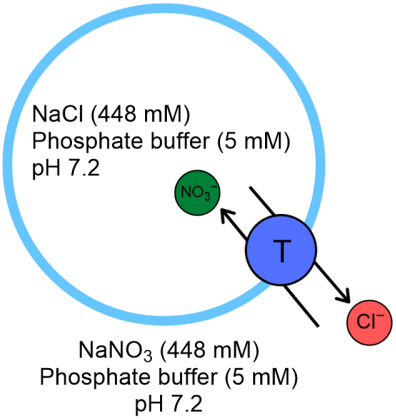

Figure 3 Schematic of the Cl^-/NO_3^- exchange assay, monitored by chloride-ISE. POPC vesicles were loaded with phosphate (5 mM) buffered NaCl (448 mM) and then suspended in phosphate (5 mM) buffered $NaNO_3$ (448 mM) and adjusted to pH 7.2.

Table 2. EC_{50} values and Hill coefficients (n) from the Cl^-/NO_3^- exchange assay, maximum transport rate at a 0.05 mol% loading of the transporter, and calculated lipophilicity values (clog *P*) are displayed for the transporters.

Compound	EC_{50} (mol%) [a]	n	Maximum rate (% s^{-1}) [b]	clog *P* [c]
3	0.0011	1.3	21.9 [d]	3.96
4	0.0068	1.0	1.01	6.41
5	0.025	3.1	0.27 [e]	- [f]
8	0.042	3.0	0.56	4.73
9	0.064	2.6	0.28	7.08
10	0.14	2.0	0.07[e]	- [f]

[a] EC_{50} at 270 s, shown as receptor:lipid molar percent. [b] Maximum initial rate calculated at a loading of 0.05 mol%, by fitting efflux plot to an exponential decay function. [c] Average clog *P* values calculated using VCCLab.[26,27] [d] Initial rate calculated at 0.01 mol%. [e] Efflux plot fit to Boltzmann sigmoidal curve. [f] clog *P* could not be reliably calculated.

Bis-urea compounds **3**–**5** were found to be considerably more active than their thiourea analogues **8**–**10**, in contrast to trends previously observed for many families of anionophores.[28-30] Typically, sulfur atoms enhance the acidity of the thiourea NH protons relative to the urea oxygen atoms, which leads to stronger coordination of a chloride anion and enhanced lipophilicity, allowing more efficient diffusion from the water/membrane interface. The EC_{50} values can again be rationalised by considering the planarity afforded in the 1:1 binding mode of the bis-urea compounds (molecular modelling can be viewed in the supplementary information, Figure S149). The planar conformation offers a more complete encapsulation of a bound chloride anion and better shielding of the negative charge from the polar head groups of the lipid bilayer. Additionally, the bis-urea oxygens are held almost parallel to the acridinone plane due to the presence of intramolecular hydrogen bonds. The 1:1 binding mode of the thioureas is distorted due to the bulk of the sulfur atoms (Figure S150). The bound chloride anion is more exposed to the external environment, and the bis-thiourea sulfur atoms sit almost perpendicular to the acridinone plane. The sulfur atoms are also exposed to the polar phospholipid head groups and the non-polar bilayer interior, making transport less efficient. A similar conformation was observed for the anthracene-based bis-(thio)urea transporters which was attributed to the instability of the thiourea compounds in solution.[7] The acridinone bis-thiourea compounds in DMSO solution were found to slowly decompose but this does not happen on the time scale of the transport experiments. The potential for tautomerism of the bis-urea receptors to occur during the transport process cannot be discounted.

The beneficial effect of strongly electron-withdrawing groups on transport activity is apparent for both the bis-urea and bis-thiourea series of receptors. *para*-NO_2 and 3,5-CF_3 groups increased the binding affinity of the (thio)urea groups towards chloride, shown in Table 1 and also facilitate a greater degree of delocalisation of the negative charge around the molecule, thereby enhancing the lipophilicity of the receptor:guest complex.[31] Compounds **3** and **4** are highly effective chloride transporters. The EC_{50} value calculated for compound **3** of 0.0011 mol% ranks it among the most effective transporters reported by our group. For comparison, the most potent *ortho*-

Please do not adjust margins

Please do not adjust margins

phenylenediamine-based transporter has a EC_{50} value of 0.0015 mol% in the Cl^-/NO_3^- exchange assay.[32] Measurable activity was observed for compound **3** at transporter to lipid loadings as low as 1:500000 transporter:lipid ratio (2 *n*M in the aqueous suspension, or 0.0002 mol%), as shown in Figure 4.

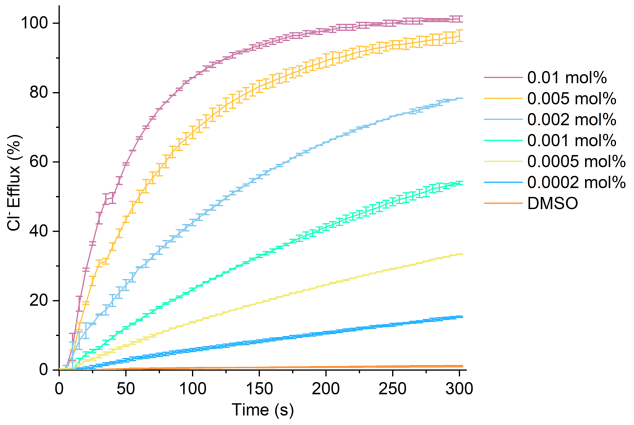

Figure 4. Dose response studies for compound **3** using the Cl^-/NO_3^- ISE assay. Each data point is the average of two repeats with error bars to show standard deviation. A run of pure DMSO was used as a control.

A Hill coefficient of close to n = 1 was determined for receptors **3** and **4**, indicating that these compounds transport Cl^- in a 1:1 host:guest stoichiometry. The Hill coefficient for the other compounds (**5**, **8**–**10**) was determined to be n ≥ 2, suggesting a higher stoichiometry is required to facilitate transport. The distorted binding site present in bis-thiourea compounds **8**–**10** may leave a bound chloride anion too exposed to the lipid bilayer interior. A requirement of at least two bis-thiourea molecules to successfully shield the negative charge is another potential explanation for the poorer transport activity displayed by the bis-thiourea compounds in this assay compared to their bis-urea analogues.

The rates of chloride efflux achieved by receptors **4**, **5** and **8**–**10** were calculated from the efflux plots at a transporter loading of 0.05 mol%, to offer comparison across the series, and are shown in Table 2. The high activity of compound **3** in the Cl^-/NO_3^- exchange assay allowed the determination of the maximum transport rate to be calculated at a lower transporter loading of 0.01 mol%. The transport rate values of compounds **3**–**4** and **8**–**9** were obtained by fitting the respective efflux plots to an exponential decay function and calculating the initial rate. The trend in rates for these compounds is concordant with the calculated EC_{50} values, and the rate of transport facilitated by compound **3** was significantly higher than the other compounds tested even at a lower loading. The efflux plots at 0.05 mol% loading of the *para*-SF_5 compounds **5** and **10** were sigmoidal in shape and were therefore fit to a Boltzmann sigmoidal curve. The maximum rate of transport calculated for these compounds occurs in the middle of the experiment, rather than at the beginning. The slow initial rate of transport exhibited by the *para*-SF_5 receptors is reflective of their poor solubility, suggesting that delivery of the transporter and its partition into the lipid bilayer may be the rate-limiting step of the transport process.

The degree of lipophilicity of compounds **3**–**4** and **8**–**9** was quantified by calculating the octanol-water partition coefficients (clog *P*) using the online VCCLab ALOGPS2.1 applet,[26] and the values are displayed in Table 2. The clog *P* values of *para*-SF_5 derivatives **5** and **10** could not be accurately calculated using the online VCCLab applet; however, it is reported extensively in the literature that these groups are more lipophilic than *para*-CF_3 compounds.[33,34] Previous research by the our group and others has demonstrated that lipophilicity is a crucial parameter dictating the transport activity of synthetic mobile carriers.[35-37] Systems that are too lipophilic cannot diffuse into the aqueous phase or pass through the barrier formed by the polar head groups, which is necessary to extract or release of an anion into the aqueous bulk. This can become the rate-limiting step of the transport process. The greater lipophilicity of bis-CF_3 receptor **4** (clog *P* = 6.41) could potentially slow its transport rate compared to compound **3**, which has a more moderate degree of lipophilicity (clog *P* = 3.96).

Cationophore coupled transport assay

The mechanism of the chloride transport processes mediated by anionophores **3**–**5** and **8**–**10** were investigated using complementary cationophore coupled assays (Figure 5). POPC vesicles were loaded with 300 mM KCl and suspended in a 300 mM solution of either potassium gluconate (KGlc) or KNO_3, buffered to pH 7.20 with potassium phosphate salts. Gluconate cannot be transported across the bilayer because it is large and polar; thus, compound-mediated Cl^- transport is dependent on coupling to either valinomycin or monensin. Both cationophores transport K^+ across the bilayer via different mechanisms and indicate different modes of Cl^- transport.

Valinomycin strictly uniports K^+, thus coupling to valinomycin indicates electrogenic transport of Cl^- facilitated by the tested transporter. In contrast to valinomycin, monensin exchanges K^+ and H^+ across the phospholipid bilayer, thus coupling to monensin is indicative of the electroneutral symport of Cl^-/H^+ out of the vesicle facilitated by the anion transporter.

Receptors were added as a DMSO solution (10 µL) at *t* = 0 and efflux of chloride was measured using a Cl^- ion-selective electrode. Detergent was added at *t* = 300 s to lyse the vesicle and provide a reading for 100% Cl^- efflux. Transport activity in KNO_3 external solution should correspond to the results of the Cl^-/NO_3^- exchange assay, whereas activity in KGlu external solution should be significantly reduced.

Experiments with a KGlc external solution were repeated in the presence of valinomycin and monensin, separately. The cationophores were added at *t* = −30 s as a DMSO solution (10 µL, 0.1 mol% loadings, with respect to lipid concentration), before transporters were added as a DMSO solution (10 µL) at *t* = 0 s. The transporter loading for each receptor was chosen to closely match the respective EC_{50} value calculated for the Cl^-/NO_3^- exchange assay.

Please do not adjust margins

Please do not adjust margins

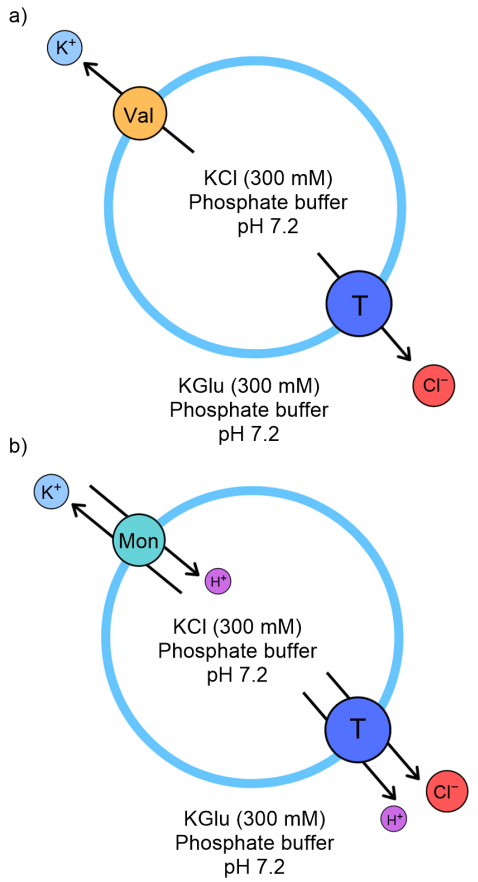

Figure 5 Schematic of the cationophore coupled KCl efflux assay, monitored by chloride-ISE. POPC vesicles were loaded with phosphate buffered KCl (300 mM) and then suspended in phosphate buffered K-Glu (300 mM) and adjusted to pH 7.2. Diagrams show a) overall KCl efflux induced by valinomycin's (Val) electrogenic K^+ transport coupled to the anionophore's electrogenic Cl^- transport resulting in an overall electroneutral KCl efflux and b) overall KCl efflux induced by monensin's (Mon) electroneutral K^+/H^+ exchange and the transporter's Cl^-/H^+ cotransport (or Cl^-/OH^- exchange).

Chloride efflux in the presence of monensin was observed in all cases, and the results for receptors **4** and **9** are shown in Figure 6. In general, only minimal Cl^- efflux was observed in the presence of valinomycin, indicating that the transporters do not function via an electrogenic Cl^- uniport mechanism. The results in the presence of monensin demonstrate that the transporters function as H^+/Cl^- cotransporters. Compounds that facilitate a symport process have been shown to have potential for cancer treatment, by creating a pH gradient in tumour cells and inducing apoptosis.[38-40]

Compounds **9** and **10** were found to couple to valinomycin; however, efflux via this pathway was slower than when the compounds were coupled to monensin. Electrogenic Cl^- transport requires the transporter molecule to diffuse back across the lipid bilayer as a neutral species after release of a chloride anion. This can be inhibited if a neutral receptor interacts strongly with phosphate headgroups in the bilayer, making them unable to diffuse across the membrane.[41, 42] Initial investigations on compound **1** in 2007 highlighted the potential for strong interactions between the receptor and phosphate.[11] It is likely that this interaction is the reason that compounds **3**–**5** and **8** are incapable of facilitating Cl^- uniport. Compounds **9** and **10** have the lowest Cl^- binding constants of the anionophores tested in the cationophore coupled assay (Table 1), and this suggests they likely also have the weakest affinity towards the headgroups. Therefore, compounds **9** and **10** can traverse the membrane as a neutral species and electrogenic Cl^- transport is permitted; albeit at a slower rate than electroneutral H^+/Cl^- cotransport.

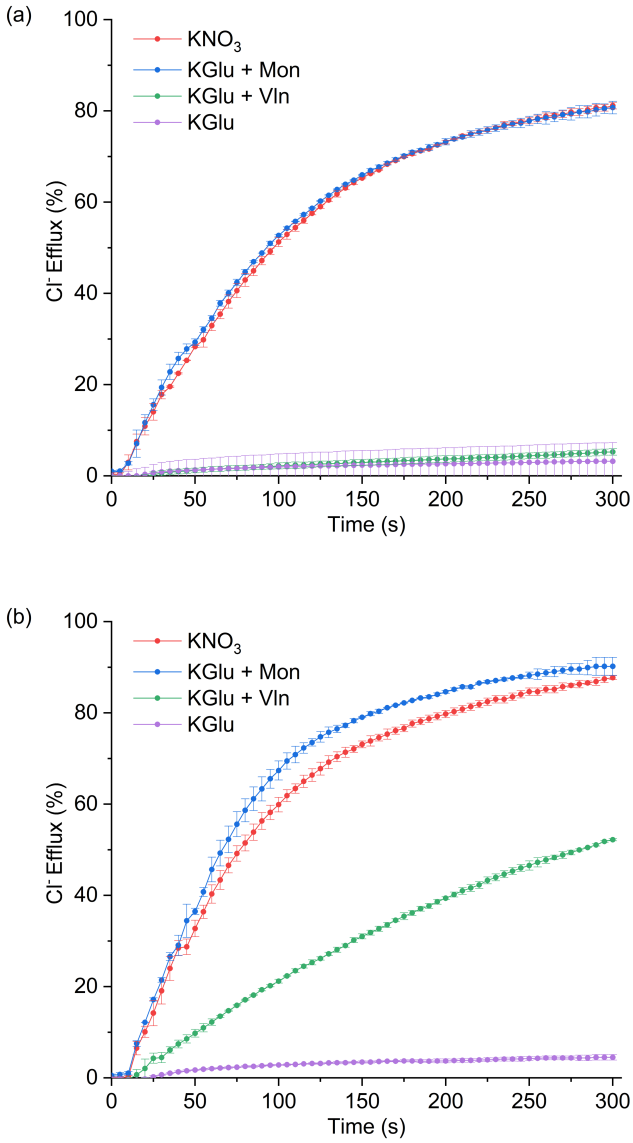

Figure 6. The chloride efflux facilitated by a) **4** (0.02 mol%) and b) **9** (0.2 mol%) in POPC vesicles loaded with KCl (300 mM) and suspended in an isotonic external solution containing KNO_3 (red) or containing KGlu (300 mM) in the presence of 0.1 mol% monensin (blue) and 0.1 mol% valinomycin (green). Each data point is the average of two repeats with the error bars showing the standard deviation. The chloride efflux from free transporter in the external KGlu solution is shown as the control (purple).

HPTS assay for HCl transport

Please do not adjust margins

Please do not adjust margins

The ability of compounds **3**–**5** and **8**–**10** to mediate electroneutral H^+/Cl^- cotransport was determined using HPTS fluorescence assays (Figure 7). Initially, dose response studies were performed, followed by Hill analysis, using a NMDG-Cl HPTS assay.[43] A lower concentration of lipids are used in these experiments (0.1 mM), meaning lower transporter concentrations are required to facilitate transport. EC_{50} values were calculated for the whole series of compounds **1**–**10** using this assay, offering a more complete picture of transport activity.

Vesicles (200 nm) were prepared with an internal solution of NMDG-Cl (100 mM), buffered with HEPES (5 mM) to pH 7.0, and containing HPTS (1 mM). The LUVs were then suspended in the same external solution of NMDG-Cl which had not been treated with HPTS. An artificial pH gradient was initiated for each experiment using a base pulse of NMDG (5 mM), before the transporter was added to the suspension as a DMSO solution (5 µL to a total volume of 2.5 mL) at t = 0 s. $NMDG^+$ is a large, hydrophilic cation that cannot be transported through the bilayer; therefore, the only process possible capable of dissipating the pH gradient is H^+/Cl^- cotransport. Changes to the intravesicular pH induced by cotransport of HCl were followed by monitoring the change in fluorescence ratio of HPTS. Detergent was added at t = 210 s to lyse the vesicles and provide a calibration reading of 100% proton efflux. EC_{50} values and Hill coefficients for compounds **1**–**10** are displayed in Table 3.

Table 3. EC_{50} values and Hill coefficients (n) for compounds **1**–**10** in the NMDG-Cl HPTS assay. EC_{50} values were calculated using the Hill equation.

Compound	EC_{50} [a]	n	clog P [b]
1	0.0077	1.2	3.72
2	0.0035	0.9	5.45
3	0.00015	0.8	3.96
4	0.0076	0.5	6.41
5	0.0055	1.1	[c]
6	0.15	1.2	4.34
7	0.014	1.3	5.79
8	0.0046	0.7	4.73
9	0.036	0.9	7.08
10	0.03	1.9	[c]

[a] EC_{50} at t = 180 s, shown as receptor:lipid molar percent (mol%). [b] Average clog P values calculated using VCCLab.[26,27] [c] clog P could not be reliably calculated.

The transport activity of the bis-urea compounds **1**–**5** in this assay compared to the bis-thiourea compounds **6**–**10** mirrored the results of the Cl^-/NO_3^- ISE exchange assay. The calculated EC_{50} values for each of the bis-urea compound were at least 4 times smaller than their bis-thiourea analogues. Compound **3** was again the most potent transporter of the series, with an EC_{50} value of 0.00015 mol%, which is a factor of 10 smaller than the other anionophores tested, adding further evidence towards the effectiveness of the NO_2 derivatives as anion transporters. Hill coefficients (n) were close to n = 1 in all cases aside from compound **10**, where the value was closer to n = 2. These findings indicate a 1:1 stoichiometry is preferred for transport under the conditions of this assay.

Interestingly, the *para*-CF_3 compounds **2** and **7** were more active in the assay than the respective 3,5-bis-CF_3 and *para*-SF_5 derivatives. Aqueous solubility is less of an issue in these studies due to the lower concentrations required to facilitate transport, therefore it seems likely that lipophilicity plays a crucial role. The presence of two additional trifluoromethyl groups in receptors **4** and **9** greatly enhances the overall lipophilicity of the respective systems, and could result in unfavourable deliverability. A similar degree of lipophilicity is expected for *para*-SF_5 derivatives **5** and **10**, and the results suggest that these compounds also exceed the optimal degree of lipophilicity required for efficient chloride transport.

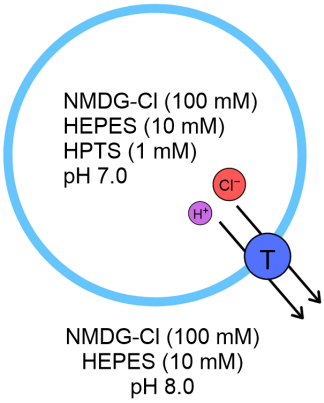

Figure 7 Schematic of the NMDG-Cl assay, monitored by HPTS fluorescence. POPC vesicles were loaded with HEPES (10 mM) buffered NMDG-Cl (100 mM) with HPTS (1 mM) and suspended in HEPES (10 mM) buffered NMDG-Cl (100 mM) and adjusted to pH 7. To start the experiment a base pulse of NMDG (0.5 M) was added to increase the external pH to pH 8.

Voltage dependent HPTS assay

A voltage-dependent KCl HPTS base pulse assay was employed to further probe the H^+/Cl^- symport mechanism facilitated by this class of anionophores (Figure 8).[41] Membrane potentials were generated by varying the intravesicular and extravesicular K^+ concentrations and introducing valinomycin at the beginning of each experiment. Two solutions of vesicles were prepared in a solution of KCl (100 mM) or a 99:1 NaCl/KCl solution (NaCl = 99 mM, KCl = 1mM) solution, buffered to pH 7.0 with HEPES (10 mM). The LUVs were then suspended in an external solution which corresponded to the generation of a neutral membrane potential, a positive membrane potential (118 mV), or a negative potential (−118 mV). Valinomycin in a DMSO solution (5 µL, 0.1 mol%) and a NaOH base pulse (5 mM) were added to the solutions at t = −30 s before the experiment was initiated with the addition of transporter in a DMSO solution (5 µL) at t = 0 s. A single dose was used for each compound at a concentration that corresponded to the EC_{50} value determined in the NMDG-Cl HPTS assay. Full experimental methods and fluorescence plots can be viewed in the supplementary information.

Please do not adjust margins

Please do not adjust margins

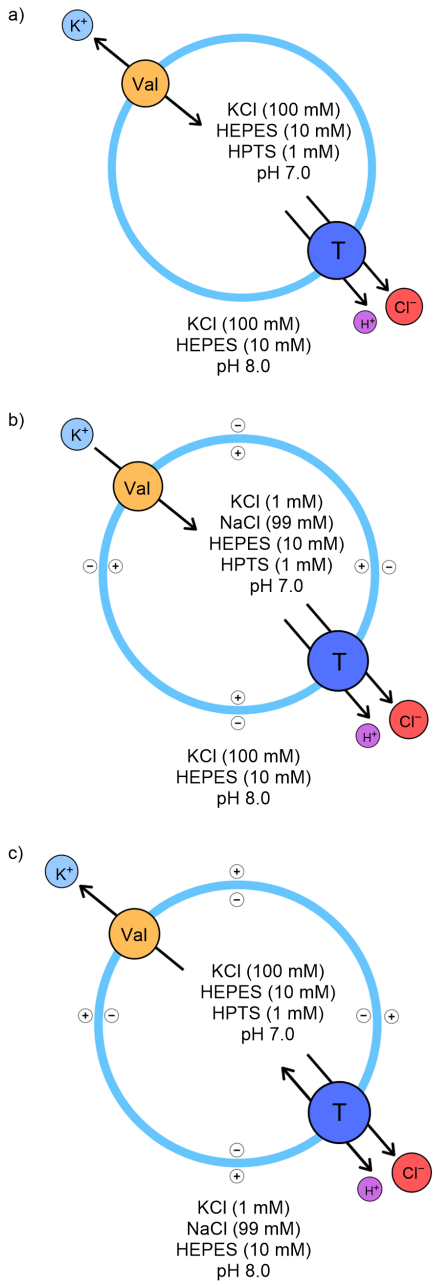

Figure 8 Schematic representation of voltage-dependent HPTS assays, showing generation of membrane potentials of 0, 118 and −118 mV using valinomycin and a K^+ gradient. All internal and external solutions are buffered by HEPES (10 mM).

There are two putative H^+/Cl^- symport mechanisms. The first involves protonation of a neutral receptor and subsequent binding of chloride as a neutral complex, followed by the diffusion of the neutral free receptors back across the membrane to complete the transport cycle. The naturally occurring anionophore prodigiosin has been shown to operate via this mechanism.[44] Transport mediated by this process should be unaffected by membrane potential, as it involves the diffusion of neutral species only. A second mechanism arises when an anionophore transports chloride as a negatively charged receptor·chloride complex and diffuses back as a negatively charged deprotonated species or complex with deprotonated fatty acids. If the anionophore cannot diffuse through the membrane as a neutral anion-free receptor due to strong binding to phosphate headgroups, symport via this mechanism should be attenuated by the generation of a membrane potential because this should inhibit the diffusion of either one of the negatively charged species or complex.

The bis-urea compounds **1**–**5** all showed an attenuation in transport rate when either a positive or negative membrane potential was applied (Figure 9a). This provides evidence that H^+/Cl^- symport is facilitated by a non-uniport mechanism, likely due to strong interactions with the phosphate headgroups as proposed in previous voltage-dependent transport studies.[45] The possibility of tautomerism of the deprotonated form of the receptor may also favour this mechanism, as this would delocalise the negative charge over a greater portion of the molecule and allow it to diffuse through the membrane more easily.

Compound **8** displayed similar voltage-dependent transport to the bis-urea compounds, however, the other thiourea compounds behaved differently under the conditions of the assays. Compounds **6** and **9** (Figure 9b) facilitated pH dissipation at a faster rate in the presence of a positive membrane potential, and when a negative membrane potential was applied the intravesicular solution became acidified. These findings suggest that compounds **6** and **9** can function as H^+ uniporters in the presence of valinomycin, because their neutral free receptor form is able to freely diffuse across the membrane which may be a consequence of weaker interactions with the phosphate headgroups.

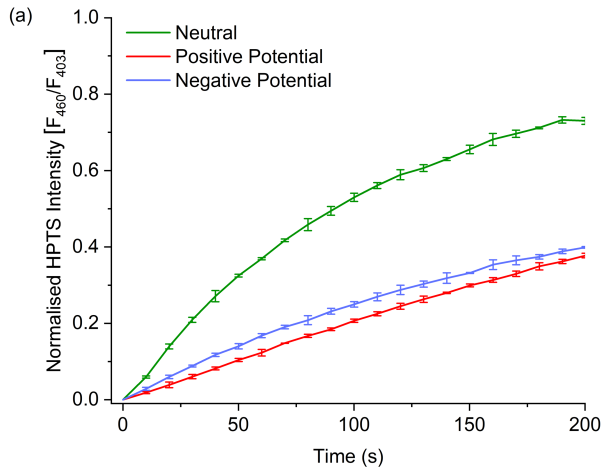

Please do not adjust margins

Please do not adjust margins

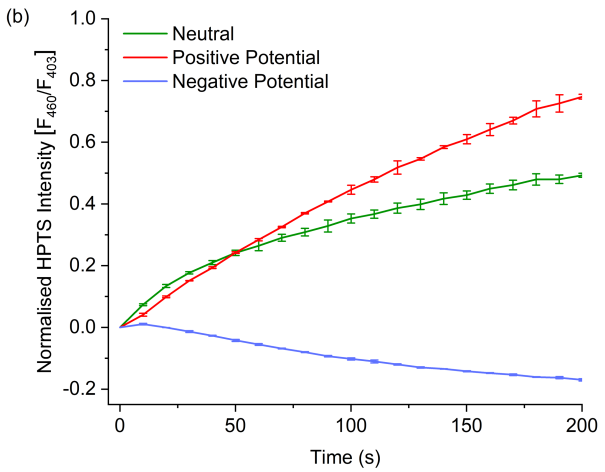

Figure 9. Voltage-dependent HPTS base pulse assay efflux plots for a) **3** (0.05 mol%) and b) **9** (0.02 mol%) at a neutral membrane potential (green), a positive membrane potential (red), and negative membrane potential (blue), generated using valinomycin based on a K^+ concentration gradient. Each data point is the average of two repeats with the error bars showing the standard deviation.

Mechanistic studies

Additional experiments were undertaken to identify the proton transport mechanism, and the influence of fatty acids in the lipid bilayer on the rate of transport (Figure 10). POPC vesicles were prepared with a solution of NaCl (100 mM) and HPTS (1mM), buffered to pH 7.0 with HEPES (5 mM). The vesicles were suspended in an identical external solution which was prepared without the presence of HPTS. A pH gradient was induced with a NaOH base pulse (5 mM) and transporter was added to the experiment as a DMSO solution (5 µL to a total volume of 2.5 mL) at t = 0 s. A single dose was used for each compound corresponding to the concentration used in the voltage dependent HPTS assays. The experiments were repeated in the presence of carbonyl cyanide-m-chlorophenylhydrazone (CCCP), with the protonophore being added at $t = -30$ s.

In the presence of CCCP, transport experiments can identify whether there is a $Cl^- > H^+$ selectivity in the transport process. An increase in the rate of transport in the presence of CCCP indicates that the transport of protons is the rate-limiting step. An acceleration in pH dissipation was not observed for compounds **1**–**10** in the presence of CCCP and, in some cases, a decrease in the rate of transport was observed (Figure 11). To couple to CCCP, a transporter must be able to facilitate electrogenic chloride uniport. These results are further evidence that the acridinone-based compounds do not facilitate transport by this mechanism.

Subsequently, the vesicles were treated with bovine serum albumin (BSA) and stirred vigorously for three hours to remove trace fatty acids from the lipid bilayer. Transport experiments were repeated, and a decrease in the rate of pH dissipation compared to the non-treated vesicles was observed in all cases (Figure 11). The decrease in the rate of pH dissipation in the absence of membrane fatty acids suggest that the transporters facilitate a fatty acid-dependent pH dissipation pathway. Fatty acids deprotonate to release protons into the extravesicular solution and then a transporter molecule can bind to the carboxylate headgroup to mediate its transport through the bilayer to the vesicle interior. The carboxylate is then reprotonated by the intravesicular solution and can flip back to the vesicle exterior as a neutral species, thereby completing the H^+ transport cycle.

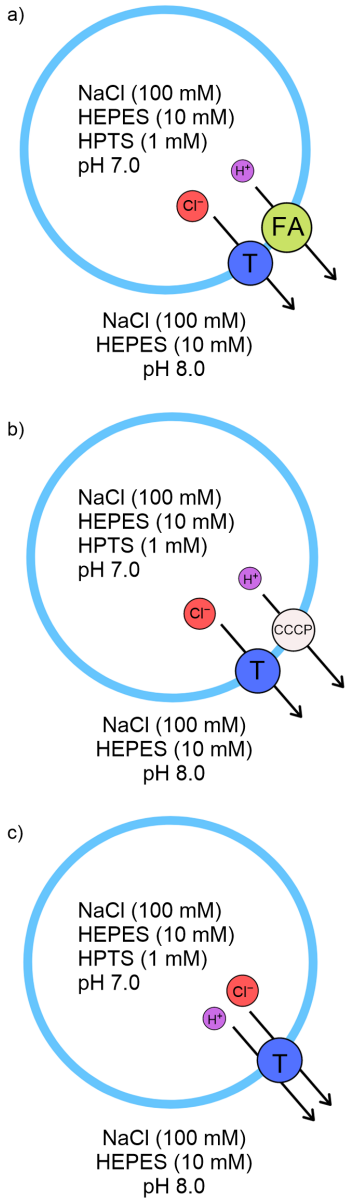

Figure 10 Schematic of the KCl assay, monitored by HPTS fluorescence. a) Overall pH dissipation from the transporter facilitating Cl^-/H^+ cotransport via chloride transport and facilitating fatty acid flip-flop, b) overall pH dissipation resulting from the transporter facilitating Cl^- transport coupled with the weak acid protonophore CCCP, which facilitates H^+ efflux, and c) overall pH dissipation resulting from the transporter facilitating HCl co-transport.

Please do not adjust margins

Please do not adjust margins

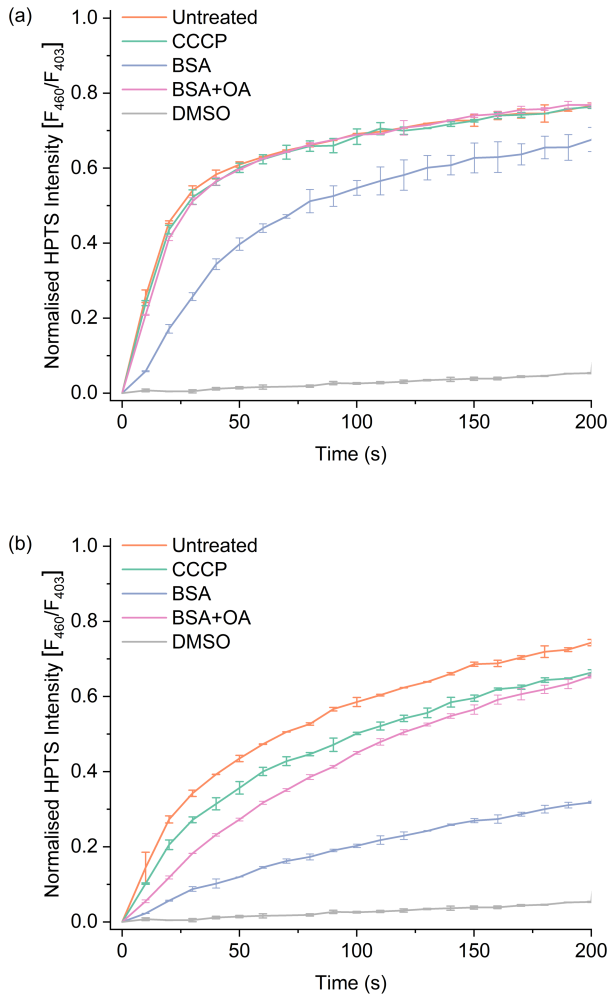

Figure 11 HPTS fluorescence for a) **4** (0.01 mol%) and b) **9** (0.02 mol%) as a free receptor (orange), in the presence of CCCP (green), in BSA-treated vesicles (blue) and in BSA-treated vesicles in the presence of OA (pink). A DMSO blank (grey) was used as a control.

The propensity to facilitate this process was further evidenced after the addition of oleic acid (OA) to the BSA-treated vesicles, which resulted in an increase in pH dissipation rate for all compounds tested (Figure 11). This means the H^+/Cl^- symport process can be at least partially ascribed to a fatty acid-dependent pathway. The findings in the cationophore coupled assay indicate that the transporters, after releasing chloride, must deprotonate before moving back through the lipid bilayer due to strong interactions with the phospholipid headgroups in their charge-neutral form. However, this process can be expedited by binding a neutral transporter molecule to a deprotonated fatty acid, which then moves through the lipid bilayer as a complex. This offers an alternative H^+/Cl^- symport pathway, and accounts for the reduction in the transport rate when trace fatty acids are removed.

Anion transport selectivity studies

Recently, we have reported the suitability of 'anion gradient' assays for determining the selectivity of a transporter towards chloride over other anions (Figure 12).[45] Vesicles were prepared in a solution of NaCl (100 mM) and HPTS (1 mM), buffered to pH 7.0 with HEPES (10 mM). Following this procedure, the vesicles were suspended in external solutions of NaX (100mM), also buffered to pH 7.0, where $X^- = Cl^-, Br^-, NO_3^-, I^-$, or ClO_4^-. No base pulse was added, and the experiment was initiated by the addition of a transporter as a DMSO solution (5 µL to a total volume of 2.5 mL) at t = 0 s. Selectivity is determined by observing the maximum ΔpH values reached during each experiment. If the rate of HCl efflux exceeds the rate of HX influx, then the intravesicular solution is basified, and ΔpH will be a positive value. If the rate of HX influx is the faster process then protons will enter the vesicles at a quicker rate than protons leaving through HCl efflux, and therefore the ΔpH value should be negative. To exhibit chloride-selective transport, a compound must return a positive ΔpH value against the other anions tested.

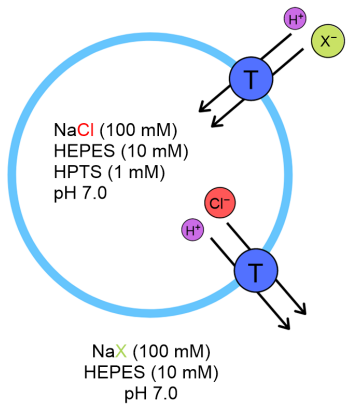

Figure 12 Schematic showing the general conditions required for the anion gradient assay. X = $Cl^-, Br^-, NO_3^-, I^-, ClO_4^-$. If the transport rate of HCl > HX, then the vesicle interior is basified. If the transport rate of HCl < HX, then the vesicle interior is acidified.

The transport selectivity for compounds **1–10** generally followed the order $I^- > Br^- > Cl^- > NO_3^- > ClO_4^-$. The trend for the halide anions follows the sequence predicted by the Hofmeister series, with the transport of more hydrophobic anions facilitated more efficiently. Interestingly, all compounds transported chloride at a faster rate than NO_3^- and ClO_4^-, despite the higher lipophilicity of the two anions. It is likely that the preorganised, convergent bis-(thio)urea binding site is a better geometrical match for spherical halide anions over the more complex geometries of NO_3^- and ClO_4^-. A similar $Cl^- > NO_3^-$ transport selectivity was previously observed for tren-based thiourea compounds,[45] and therefore the transport of NO_3^- is the rate-limiting step in the Cl^-/NO_3^- assay for these compounds. Therefore, the true Cl^- transport activity achieved by compounds **3–5** and **8–10** may have been underestimated due to poor transport of NO_3^-.[46] Notably, compound **4** exhibited minimal transport selectivity for Br^- over Cl^-, and the negative ΔpH value afforded by an external solution of HI was also small (Figure 13). By comparison, the bis-thiourea analogue **9** showed considerable $I^- > Cl^-$ selectivity (Figure 14). The tight, planar binding site afforded by the bis-urea groups, coupled with the

Please do not adjust margins

Please do not adjust margins

steric bulk of the 3,5-bis-CF_3 substituents, creates the most Cl^- size-selective binding site of the series.

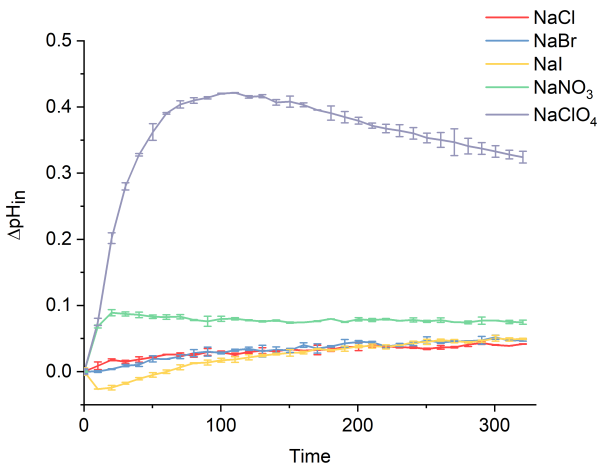

Figure 13 The anion selectivity assay for **4** (0.01 mol%, added at time 0). Initial conditions: In: NaCl (100 mM), HPTS (1 mM), HEPES (10 mM), pH 7.0; Out: NaX (100 mM), HEPES (10 mM), pH 8.0. [POPC] = 0.1 mM, [DMSO] = 5 µL. Error bars represent the standard deviations from two runs.

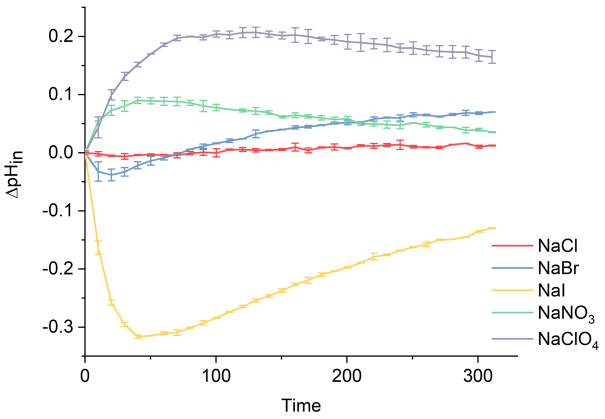

Figure 14 The anion selectivity gradient assay for **9** (0.02 mol%, added at time 0). Initial conditions: In: NaCl (100 mM), HPTS (1 mM), HEPES (10 mM), pH 7.0; Out: NaX (100 mM), HEPES (10 mM), pH 8.0. [POPC] = 0.1 mM, [DMSO] = 5 µL. Error bars represent the standard deviations from two runs.

Experimental

General Experimental Methods

Anhydrous solvents were collected from an Inert Corp PureSolv MD7 solven purification system. Deionised water was collected from a Merck Millipore Milli-Q™ reference ultrapure water purification system.

The nuclear magnetic resonance (NMR) spectra were recorded at 300 K using a Bruker AVIII 500, Bruker Avance DPX 400, or a Bruker Avance 600 spectrometer. ^{1}H and ^{13}C NMR spectra were recorded at the indicated frequency, and calibrated to the residual DMSO-d_6 solvent peak (δ = 2.50 ppm and δ = 39.52 ppm, respectively). The resonances are reported as chemical shifts in ppm, multiplicity, coupling constant in Hz, and by their relative integral. Melting points were recorded manually using a Standford Research Systems Optimelt machine, and data were reported as a range (°C). Low resolution mass spectrometry was performed with a Bruker amaZon SL mass spectrometer using electrospray ionisation. High resolution mass spectra were recorded on a Bruker Apex II Fourier Transform Ion Cyclotron Resonance (FTICR) mass spectrometer with a 7.0 T magnet, fitted with an off-axis analytic electrospray source with quadrupole mass analyser, and are reported as m/z (relative intensity).

To prepare the vesicles, a chloroform solution of POPC (37.5 mM, 4 mL) was transferred to a pre-weighed round-bottom flask, and the solvent was removed using a rotary evaporator. The pressure was lowered slowly to ensure the formation of a smooth lipid film. Subsequently, the film was dried *in vacuo* for 4–24 h, and the mass of lipid was recorded. The lipids were rehydrated with 4 mL of the respective internal solution (this number should correspond to the volume of POPC solution used initially) and vortexed until all lipids were removed from the sides of the flask and were suspended in solution. The lipids were subjected to 9 cycles of freeze-thaw by freezing using a dry ice/acetone bath and thawing in lukewarm water. Following this, the vesicles were left to rest at room temperature for 30 min. The lipids were extruded through a 200 nm polycarbonate membrane 25 times to form monodisperse vesicles. Only 1 mL of solution was extruded at a time before being collected. Finally, any residual unencapsulated salt from the internal solution was either removed via dialysis for 12 h in the desired external solution or through size-exclusion using a B19 column packed with hydrated G-25 Sephadex®, which had been pre-saturated with the respective external solution. The lipid suspensions were diluted with the external solution to afford a stock solution (10 mL) of a known concentration. The ISE assayd were conducted on the Fisherbrand™ Accumet™ Chloride Combination Electrode, and the HPTS transport fluorescence data was recorded on an Agilent Cary Eclipse Fluorescence Spectrophotometer.

1,9-Bisphenylurea-9(10H)-acridinone (1)

Compound **1** was synthesised using a literature procedure.[11] 1,9-Diaminoacridinone (100 mg, 0.44 mmol) was dissolved in dry DMF (5 mL) and stirred under nitrogen. Separately, phenyl isocyanate (0.15 mL, 1.33 mmoL) was dissolved in DMF (1 mL) and added dropwise to the first solution. This reaction was left for 3 h, by which time a light brown precipitate had formed. This precipitate was filtered, suspended, and sonicated in 1:1 v/v diethyl ether/hexane (100 mL) for 30 min and then filtered again. This was washed with further portions of diethyl ether (3 x 30 mL) before being dried *in vacuo* to yield a brown solid (127.5 mg, 0.27 mmol, 62%). Analytical data matched that of this compound in the literature.

Mp = 361–364 °C (decomposition)

^{1}H NMR (500 MHz, DMSO-d_6) δ ppm 10.65 (1 H, s), 8.9 (2 H, s), 8.74 (2 H, s), 8.13 (2 H, d, J 7.6), 7.69 (2 H, d, J 6.7), 7.42 (4 H, d, J 7.2), 7.3 (2 H, d, J 7.5), 7.14 (4 H, t, J 7.8), 6.94 (2 H, t, J 7.1); **^{13}C{^{1}H} NMR** (101 MHz, DMSO-d_6) δ ppm 177.4, 154.4, 139.8, 136.1, 129.7, 129.1, 127.6, 123.5, 122.0, 121.6, 119.1.

LR-MS (ESI$^-$) *m/z* 498.22 [M−H]$^-$; **HR-MS** (ESI$^+$) calcd for $C_{27}H_{21}N_5O_3$ [M+H]$^+$: 464.17172, found *m/z* 464.17164.

1,9-Bis(4-(trifluoromethyl)phenyl)urea-9(10H)-acridinone (2)

1,9-Diaminoacridinone (50 mg, 0.22 mmol) was dissolved in DMSO (3 mL). 4-(Trifluoromethyl)phenyl isocyanate (0.11 mL, 0.78 mmol) was added dropwise, and the reaction left to stir for 15 min. Next, the solution was poured onto ice-cold deionised

Please do not adjust margins

Please do not adjust margins

water (25 mL) and a precipitate formed, which was filtered. This precipitate was then washed with water (3 x 30 mL), hexane (3 x 15 mL), and suspended in 1:1 v/v ethyl acetate/hexane (50 mL) before being sonicated for 30 min. The solid was again filtered, washed with a further portion of 1:1 50% ethyl acetate/hexane, then dried *in vacuo* (83 mg, 0.14 mmol, 63%).

Mp = 333−336 °C (decomposition)

^{1}H NMR (600 MHz, DMSO-d_6) δ ppm 10.50 (1 H, s), 9.4 (2 H, s), 8.91 (2 H, s), 8.15 (2 H, dd, J 8.1, 1.5), 7.68 (2 H, dd, J 7.6, 1.5), 7.56 (4 H, d, J 8.5), 7.35 (4 H, d, J 8.7), 7.31 (2 H, t, J 7.8); **^{13}C{^{1}H} NMR** (101 MHz, DMSO-d_6) δ ppm 176.9 (s), 153.6 (s), 143.1 (s), 135.7 (s), 129.6 (s), 126.7 (s), 125.8 (s), 124.4 (d), 123.2 (s), 121.9 (d), 121.5 (s), 121.2 (s), 117.9 (s). note Lack of definition and peak overlap restricted process of quarter splitting. **LR-MS** (ESI$^-$) *m/z* 598.19 [M−H]$^-$; **HR-MS** (ESI$^+$) calcd for $C_{29}H_{19}F_6N_5O_3$ [M+H]$^+$: 600.14649, found *m/z* 600.14625.

1,9-Bis(4-nitrophenyl)urea-9(10H)-acridinone (3)

1,9-Diaminoacridinone (50 mg, 0.22 mmol) and 4-nitrophenyl isocyanate (80 mg, 0.49 mmol) were dissolved in DMSO (3 mL). The reaction was left to stir for 15 min. Next, the solution was poured onto ice-cold deionised water (25 mL) and a precipitate formed, which was filtered. This precipitate was then washed with water (3 x 30 mL), hexane (3 x 15 mL), and suspended in hot methanol (200 mL) before being sonicated for 30 min. The solid was again filtered, washed with copious amounts of boiling methanol then dried *in vacuo*. (35 mg, 0.063 mmol, 29%).

Mp = 328−331 °C (decomposition)

^{1}H NMR (600 MHz, DMSO-d_6) δ ppm 10.18 (1 H, s), 9.66 (1 H, s) 8.97 (1H, s), 8.17 (2 H, d, 8.2), 7.90 (4H, d, 8.6), 7.68 (2 H, 2, 7.6), 7.55 (4 H, d, 8.8), 7.32 (2 H, m); **^{13}C{^{1}H} NMR** (101 MHz, DMSO-d_6) δ ppm 176.8, 153.3, 146, 140.9, 135.7, 130.0, 126.2, 124.7, 123.6, 121.5, 121.2, 117.4.

LR-MS (ESI$^-$) *m/z* 588.21 [M+Cl]$^-$; **HR-MS** (ESI$^+$) calcd for $C_{27}H_{21}N_7O_7$ [M+H]$^+$: 554.14187, found *m/z* 554.14146.

1,9-Bis(3,5-bis-(trifluoromethyl)phenyl)urea-9(10H)-acridinone (4)

1,9-Diaminoacridinone (50 mg, 0.22 mmol) was dissolved in DMSO (3 mL). Separately, 3,5-bis(trifluoromethyl)phenyl isocyanate (0.15 mL, 0.889 mmol) was dissolved in DMSO (2 mL), and this was added dropwise to the reaction mixture. The reaction was left to stir for 15 min. Next, the solution was poured onto ice-cold deionised water (25 mL), and a green precipitate formed, which was filtered. This precipitate was then washed with water (3 x 30 mL) and hexane (3 x 15 mL). The solid was washed with a further portion of 1:1 v/v diethyl ether/hexane solution and dried *in vacuo* to give a light green powder (90 mg, 0.12 mmol, 55%).

Mp = 189−192 °C

^{1}H NMR (600 MHz, DMSO-d_6) δ ppm 10.04 (1 H, s), 9.67 (2 H, s), 9.05 (2 H, s), 8.17 (2 H, dd, J 8.3, 1.5), 7.95 (4 H, d, J 1.7), 7.67 (2 H, dd, J 7.6, 1.4), 7.38 (2 H, t, J 1.7), 7.32 (2 H, t, J 7.8); **^{13}C{^{1}H} NMR** (101 MHz, DMSO-d_6) δ ppm 176.8, 153.4, 141.5, 135.6, 130.2 (dd, J 65.8, 33.1), 130.0, 126.1, 123.8, 123.1 (q, J 272.5), 121.5, 121.2, 117.3, 114.1.

LR-MS (ESI$^+$) *m/z* 758.19 [M+Na]$^+$; **HR-MS** (ESI$^+$) calcd for $C_{31}H_{17}F_{12}N_5O_3$ [M+Na]$^+$: 758.10320, found *m/z* 758.10303.

1,9-Bis(4-(pentafluorosulfanyl)phenyl)urea-9(10H)-acridinone (5)

This synthesis was adapted from a literature procedure.[47] A solution of 4- pentafluorosulfanylaniline (150 mg, 0.67 mmol) in toluene (15 mL) was treated with triphosgene (135 mg, 0.44 mmol). Immediately, triethylamine (0.16 mL, 1.18 mmol) was added, and the reaction mixture stirred at 70 °C for 2 h. After this, pentane (1 mL) was added to elicit the formation of a white precipitate. This was filtered off and the pentane removed *in vacuo* to give 4-(pentafluorosulfanyl)phenyl isocyanate dissolved in toluene, which was used immediately in the next reaction. 1,9-Diaminoacridinone (50 mg, 0.22 mmol) was dissolved in DMSO (5 mL) and added to the reaction mixture. This was stirred for 3 h and, following this, the toluene was removed *in vacuo*. Next, the DMSO solution was poured into ice water (30 mL) to yield a light brown precipitate. This was washed with a small amount of 1:1 v/v ethyl acetate:hexane solution (5 mL) followed by copious amounts of 1:1 v/v diethyl ether:hexane solution to leave a dark brown solid, which was dried *in vacuo* (99 mg, 0.14 mmol, 63%).

Mp = 259−262 °C (decomposition)

^{1}H NMR (500 MHz, DMSO-d_6) δ ppm 10.52 (1H, s), 9.48 (2H, s), 8.90 (2H, s), 8.16 (2 H, d, J 8.1), 7.66 (2 H, d, J 7.4), 7.54 (8H, m), 7.31 (2H, t, J 7.8); **^{13}C{^{1}H} NMR** (101 MHz, DMSO-d_6) δ ppm 177.3, 154.0, 143.3, 136.2, 130.2, 127.0, 126.9, 123.9, 122.0, 121.7, 118.1. (SF_5 α-carbon is not visible due to quintet splitting)

LR-MS (ESI$^+$) *m/z* 738.20 [M+Na]$^+$; **HR-MS** (ESI$^+$) calcd for $C_{27}H_{16}F_{10}N_5O_3S_2$ [M+Na]$^+$: 738.06618, found *m/z* 738.06477.

1,9-Bisphenylthiourea-9(10H)-acridinone (6)

This compound was synthesised from a literature procedure.[11] 1,9-Diaminoacridinone (100 mg, 0.44 mmol) was dissolved in dry DMF (14 mL) and stirred under nitrogen. Separately, phenyl isothiocyanate (1.05 mL, 8.8 mmol) was dissolved in dry DMF, and this was added dropwise to the first solution. This reaction was stirred for 3 h before the solvent was removed. The resultant solid was treated with 1:1 v/v diethyl ether/hexane (100 mL), sonicated for 20 min and filtered. The resultant solid was washed with portions of diethyl ether (3 x 20 mL) and methanol (3 x 20 mL) to leave a yellow solid. This was then dried *in vacuo* to yield the final compound (117 mg, 0.24 mmol, 54%). Analytical data matched that of this compound in the literature.

Mp = 297−300 °C (decomposition)

^{1}H NMR (500 MHz, DMSO-d_6) δ ppm 10.11 (2 H, s), 9.79 (2 H, s), 9.19 (1 H, s), 8.19 (2 H, d, J 7.9), 7.67 (2 H, d, J 7.2), 7.51 (4 H, d, J 7.6), 7.31 (2 H, d, J 7.7), 7.27 (4 H, t, J 7.5), 7.13 (2 H, t, J 7.1); **^{13}C{^{1}H} NMR** (101 MHz, DMSO-d_6) δ ppm 181.9, 177.4, 139.5, 137.2, 133.5, 128.9, 128.1, 125.4, 125.1, 125.0, 121.8, 121.6.

LR-MS (ESI$^+$) *m/z* 518.13 [M+Na]$^+$; **HR-MS** (ESI$^+$) calcd for $C_{27}H_{21}N_5OS_2$ [M+Na]$^+$: 518.10797, found *m/z* 518.10826.

1,9-Bis(4-(trifluoromethyl)phenyl)thiourea-9(10H)-acridinone (7)

1,9-Diaminoacridinone (65 mg, 0.29 mmol) and 4-(trifluoromethyl)phenyl isothiocyanate (196 mg, 0.64 mmol) were dissolved in DMSO (3 mL). The reaction was left to stir for 15 min. Next, the solution was poured onto ice-cold deionised water (25 mL) and a precipitate formed, which was filtered. This

Please do not adjust margins

Please do not adjust margins

precipitate was then washed with water (3 x 30 mL) and dried *in vacuo*. Next, the compound was washed with hexane (3 x 15 mL), and 1:1 *v/v* diethyl ether/hexane mixture (3 x 15 mL) and then dried *in vacuo* (103 mg, 0.16 mmol, 56%).

Mp = 218−221 °C

^{1}H NMR (500 MHz, DMSO-d_6) δ ppm 10.43 (2 H, s), 10.03 (2 H, s), 9.14 (1 H, s), 8.22 (2 H, dd, J 8.2, 1.5), 7.72 (4 H, d, J 8.3), 7.68 (2 H, dd, J 7.5, 1.2), 7.49 (4 H, d, J 8.4), 7.33 (2 H, t, J 7.8); **^{13}C{^{1}H} NMR** (101 MHz, DMSO-d_6) δ ppm 181.2, 176.9, 142.8, 136.6, 133.0, 127.3, 125.4, 125.0, 124. 4 (q, J 32.1), 124.2 (q, J 271.5), 123.5, 121.4, 121.3.

LR-MS (ESI$^-$) *m/z* 630.29 [M−H]$^-$; **HR-MS** (ESI$^+$) calcd for $C_{29}H_{19}F_6N_5OS_2$ [M+H]$^+$: 632.10080, found *m/z* 632.10069.

1,9-Bis(4-nitrophenyl)thiourea-9(10H)-acridinone (8)

1,9-Diaminoacridinone (50 mg, 0.22 mmol) and 4-nitrophenyl isothiocyanate (200 mg, 1.11 mmol) were dissolved in DMSO (3 mL). The reaction was left to stir for 15 min. Next, the solution was poured onto ice-cold deionised water (25 mL) and a precipitate formed, which was filtered. This precipitate was then washed with water (3 x 30 mL), hexane (3 x 15 mL), and suspended in diethyl ether (100 mL) before being sonicated for 30 min. The solid was again filtered, washed with another portion of diethyl ether then dried *in vacuo* (55 mg, 0.094 mmol, 42%).

Mp = 137−140 °C

^{1}H NMR (500 MHz, DMSO-d_6) δ ppm 10.63 (2 H, s), 10.17 (2 H, s), 9.07 (1 H, s), 8.23 (2 H, d, J 8.9), 7.98 (4 H, d, J 9.0), 7.77 (4 H, d, J 9.0), 7.68 (2 H, d, J 7.3), 7.34 (2 H, t, J 7.9); **^{13}C{^{1}H} NMR** (101 MHz, DMSO-d_6) δ ppm 180.9, 176.8, 145.6, 142.4, 136.4, 132.8, 127.1, 125.1, 124.0, 122.0, 121.4.

LR-MS (ESI$^+$) *m/z* 586.14 [M+H]$^+$; **HR-MS** (ESI$^+$) calcd for $C_{27}H_{19}N_7O_5S_2$ [M+H]$^+$: 586.09618, found *m/z* 586.09567.

1,9-Bis(3,5-bis-(trifluoromethyl)phenyl)thiourea-9(10H)-acridinone (9)

1,9-Diaminoacridinone (50 mg, 0.22 mmol) was dissolved in DMSO (3 mL). Separately, 3,5-bis(trifluoromethyl)phenyl isothiocyanate (144.52 mg, 0.533 mmol) was dissolved in DMSO (2.5 mL), and this was added dropwise to the reaction mixture. The reaction was left to stir for 15 min. Next, the solution was poured onto ice-cold deionised water (25 mL), and a yellow/green precipitate formed, which was filtered. This precipitate was then washed with water (3 x 30 mL) and hexane (3 x 15 mL). Next, the solid suspended in a 1:9 v/v diethyl ether/hexane mixture and sonicated for 30 mins. This was filtered, washed with further portions of 10% diethyl:ether:hexane solution, and dried *in vacuo* to give the final light yellow solid (75 mg, 0.098 mmol, 44%).

Mp = 153−156 °C

^{1}H NMR (600 MHz, DMSO-d_6) δ ppm 10.23 (2 H, s), 10.15 (2 H, s), 9.00 (1 H, s), 8.08 (2 H, d, J 8.2), 8.00 (4 H, s), 7.58 (2 H, d, J 7.5), 7.53 (2 H, s), 7.19 (2 H, t, J 7.8); **^{13}C{^{1}H} NMR** (101 MHz, DMSO-d_6) δ ppm 181.5, 176.8, 141.2, 136.3, 129.8 (q, J 33.0), 126.6, 125.2, 124.0, 123.1 (q, J 272.8), 121.6, 117.3.

LR-MS (ESI$^+$) *m/z* 790.07 [M+Na]$^+$; **HR-MS** (ESI$^+$) calcd for $C_{31}H_{17}F_{12}N_5OS_2$ [M+H]$^+$: 768.07555, found *m/z* 768.07574.

1,9-Bis(4-(pentafluorosulfanyl)phenyl)thiourea-9(10H)-acridinone (10)

4-pentafluorosulfanylaniline (410 mg, 1.86 mmol) was dissolved in dichloromethane (15 mL). Thiophosgene (0.16 mL, 2.05 mmol) was added, followed by a layer of saturated aqueous $NaHCO_3$ solution (20 mL) to trap any volatile thiophosgene. The mixture was stirred gently at room temperature for 12 h. Next, the aqueous layer was removed, and the organic layer dried with magnesium sulfate for 1 h. The solvent was removed *in vacuo*, and the resultant solid used immediately in the subsequent reaction. 1,9-Diaminoacridinone (50 mg, 0.25 mmol) and 4-(pentafluorosulfanyl)phenyl isothiocyanate (140 mg, 0.54 mmol) were dissolved in dry DMSO (2.5 mL) and stirred under N_2. This reaction was stirred for 3 h before the solvent was poured into ice water. The resultant precipitate was filtered, then treated with 1:1 v/v diethyl ether/hexane (100 mL), sonicated for 20 min and filtered. The resultant solid was washed with portions of a 1:1 *v/v* diethyl ether/hexane mixture (3 x 20 mL) to leave a green/brown solid. The solid was then dried *in vacuo* to yield the final compound (61 mg, 0.08 mmol, 33% yield).

Mp = 245−248 °C

^{1}H NMR (400 MHz, DMSO-d_6) δ ppm 10.48 (2 H, s), 10.08 (2 H, s), 9.14 (1 H, s), 8.22 (2 H, d, J 8.1), 7.7 (10 H, m), 7.33 (2 H, t, J 7.9); **^{13}C{^{1}H} NMR** (101 MHz, DMSO-d_6) δ ppm 181.7, 177.3, 148.5 (m), 143.0, 137.0, 133.5, 127.6, 126.5, 125.5, 123.5, 121.9, 121.8

LR-MS (ESI$^-$) *m/z* 783.66 [M+Cl]$^-$; **HR-MS** (ESI$^+$) calcd for $C_{27}H_{19}F_{10}N_5OS_4$ [M+H]$^+$: 748.03855, found *m/z* 748.03801.

Conclusions

A series bis-ureas and bis-thioureas appended to a central acridinone scaffold were synthesised, and their chloride binding and transport properties investigated. Compounds **3** and **4** are among the most potent transporters reported by our group to date. Extensive mechanistic studies revealed the transporters function predominantly as HCl cotransporters and diffuse back as deprotonated species or complexes with deprotonated fatty acids due to strong interactions between the phospholipid headgroups and the neutral receptors. The electroneutral HCl transport facilitated by these compounds at low-dose concentrations highlights their potential to disrupt cellular pH gradients and find application as powerful anti-cancer agents.

Author Contributions

DAM conducted the synthesis, binding, and anion transport studies. LKM conducted the crystallography and wrote the crystallography section of the paper. DAM and PAG wrote the remainder of the manuscript. PAG directed the research.

Conflicts of interest

Please do not adjust margins

Please do not adjust margins

There are no conflicts to declare.

Acknowledgements

DAM, LKM and PAG acknowledge and pay respect to the Gadigal people of the Eora Nation, the traditional owners of the land on which we research, teach and collaborate at the University of Sydney. PAG thanks the Australian Research Council (DP200100453) and the University of Sydney for funding.

Notes and references

1 J.T. Davis, P.A. Gale and R. Quesada, *Chem. Soc. Rev.*, 2020, **49**, 6056-6086; X. Wu, A.M. Gilchrist and P.A. Gale, *Chem*, 2020, **6**, 1296-1309.
2 S.-H. Park, S.-H. Park, E.N.W. Howe, J.Y. Hyun, L.-J. Chen, I. Huang, G. Vargas-Zuñiga, N. Busschaert, P.A. Gale, J.L. Sessler, I. Shin, *Chem*, 2019, **5**, 2079-2098; L.A. Jowett, E.N.W. Howe, V. Soto-Cerrato, W. Van Rossom, R. Pérez-Tomás and P.A. Gale, *Sci. Rep*., 2017, **7**, 9397; M. Perez-Hernandez, A. Arias, D. Martinez-Garcia, R. Perez-Tomas, R. Quesada, V. Soto-Cerrato, *Cancers*, 2019, **11**, 1599;S. Zhang, Y. Wang, W. Xie, E.N.W. Howe, N. Busschaert, A. Sauvat, L. Gomes-da-Silva, G. Chen, I. Martins, L. Maiuris, O. Kepp, T. Soussi, P.A. Gale, N. Zamzami and G. Kromer, *Cell Death & Disease*, 2019, **10**, 242; L. Tapia, Y. Pérez, M. Bolte, J. Casas, J. Solà, R. Quesada and I. Alfonso, *Angew. Chem. Int. Ed.* **2019,** *58*, 12465-12468.
3 R. Quesada and R. Dutzler, *J. Cystic Fibrosis*, 2020, **19**, S37-S41; A. Gianotti, V. Capurro, L. Delpiano, M. Mielczarek, M. Garcia-Valverde, I. Carreira-Barral, A. Ludovico, M. Fiore, D. Baroni, O. Mora, R. Quesada and E. Caci, *Int. J. Mol. Sci.* 2020, **21**, 1488; H. Li, H. Valkenier, A.G. Thorne, C.M. Dias, J.A. Cooper, M. Kieffer, N. Busschaert, P.A. Gale, D.N. Sheppard and A.P. Davis, *Chem. Sci.* 2019, **10**, 9663-9672; H. Li, H. Valkenier, A.G. Thorne, C.M. Dias, J.A. Cooper, M. Kieffer, N. Busschaert, P.A. Gale, D.N. Sheppard and A.P. Davis, *Chem. Sci.* 2019, **10**, 9663-9672; X. Wu, L.W. Judd, E.N.W. Howe, A.M. Withecombe, V. Soto-Cerrato, H. Li, N. Busschaert, H. Valkenier, R. Perez-Tomas, D.N. Sheppard, Y.-B. Jiang, A.P. Davis and P.A. Gale, *Chem*, 2016, **1**, 127-146; H. Li, H. Valkenier, L.W. Judd, P.R. Brotherhood, S. Hussain, J.A. Cooper, O. Jurček, H.A. Sparkes, D.N. Sheppard and A.P. Davis, *Nat. Chem.* 2016, **8**, 24-32.
4 B.A. McNally, A.V. Koulov, T.N. Lambert, B.D. Smith, J.-B. Joos, A.L. Sisson, J.P. Clare, V. Sgarlata, L.W. Judd, G. Magro and A.P. Davis, *Chem. Eur. J.* 2008, **14**, 9599-9606
5 S. J. Moore, C.J. Haynes, J. González, J.L. Sutton, S.J. Brooks, M.E. Light, J. Herniman, G.J. Langley, V. Soto-Cerrato, R. Pérez-Tomás, *Chem. Sci.,* 2013, **4**, 103-117.
6 S. Hussain, P.R. Brotherhood, L.W Judd and A.P. Davis, A. P., *J. Am. Chem. Soc.* 2011, **133**, 1614-1617.
7 C.M. Dias, H. Valkenier, and A.P. Davis, *Chem. Eur. J*. 2018, **24**, 6262-6268.
8 N. Busschaert, S.J. Bradberry, M. Wenzel, C.J.E. Haynes, J.R. Hiscock, I.L. Kirby, L.E. Karagiannidis, S.J. Moore, N.J. Wells, J. Herniman, G.J. Langley, P.N. Horton, M.E. Light, I. Marques, P.J. Costa, V. Félix, J.G. Frey and P.A. Gale, *Chem. Sci*., 2013, **4**, 3036-3045
9 N.J. Knight, E. Hernando, C.J.E. Haynes, N. Busschaert, H.J. Clarke, K. Takimoto, M. García-Valverde, J.G. Frey, R. Quesada and P.A. Gale, *Chem. Sci.,* 2016, **7**, 1600-1608.
10 P. Wang, X. Wu and P.A. Gale, *Supramol. Chem.* 2021, DOI: 10.1080/10610278.2021.1946539
11 S.E. García-Garrido, C. Caltagirone, M.E. Light and P.A. Gale, *Chem. Commun.* 2007, 1450-1452.
12 G.W. Rewcastle and W.A Denny, *Synth. Commun.* 1987, **17**, 309-317.
13 C. Caltagirone, J.R. Hiscock, M.B. Hursthouse, M.E. Light, and P.A. Gale, *Chem. Eur. J.* 2008**, 14**, 10236-10243.
14 http://supramolecular.org.
15 D.B. Hibbert and P. Thordarson, *Chem. Commun.* 2016, **52**, 12792-12805.
16 R. Faure, J-.P. Galy, E.J. Vincent, A.M. Galy, J. and Barbe, J. Elguero, *Spectroscopy Lett.* 1983, **16**, 431-439.
17 R. Faure, A. Mahamoud, J.-P. Galy, E.-J. Vincent, A.-M. Galy, and J. Barbe, *Spectroscopy Lett.* 1981, **14**, 223-238.
18 C. Gao, F. Liu, X. Luan, C. Tan, H. Liu, Y. Xie, Y. Jin, and Y. Jiang, *Bioorg. Med. Chem.* 2010, **18**, 7507-7514.
19 A. Bożyk, L. Jóźwiak, and J.Błażejowski *J. Mol. Struct.* **2002, 612**, 29-38.
20 I.-S. Han Lee and C.-K. Lee, *Bull. Korean Chem. Soc.* 2007, **28**, 1067-1069.
21 J. Elguero, C. Marzin, A.R. Katritzky and P. Linda, Advances in Heterocyclic Chemistry, Suppl. 1, in *The Tautomerism of Heterocycles.* by A.R. Katritzky and A.J. Boulton, Academic Press, New York, San Francisco, London 1976, 299.
22 A. Bożyk, L. Jóźwiak, A. Wróblewska, J. Rak, J. Błażejowski, *J. Phys. Chem. A* 2002, **106**, 3957-3963.
23 S. Issmaili, V. Pique, J.-P. Galy and R. Faure, *Mag. Res. Chem.* 1999, **37**, 591-593.
24 L.K.S. von Krbek, C.A. Schalley and P. Thordarson, *Chem. Soc. Rev.* 2017, **46**, 2622-2637.
25 L.A. Jowett and P.A. Gale, *Supramol. Chem.,* 2019, **31**, 297-312.
26 I.V. Tetko and V.Y. Tanchuk, ALOGPS 2.1 (http://www. vcclab. org) is a Free on-line Program to Predict logP and logS of Chemical Compounds.
27 I.V. Tetko, V.Y. Tanchuk, *J. Chem. Inf. Comput. Sci.* 2002, **42** 1136-45.
28 N. Busschaert, P.A. Gale, C.J.E. Haynes, M.E. Light, S.J. Moore, C.C. Tong, J.T. Davis, W.A. Harrell Jr. *Chem. Commun.* 2010, **46** 6252-6254.
29 N. Busschaert, I.L. Kirby, S. Young, S.J. Coles, P.N. Horton, M.E. Light, P.A. Gale, *Angew. Chem. Int. Ed.* 2012, **51**, 4426-4430.
30 H. Valkenier, L.W. Judd, H. Li, S. Hussain, D.N. Sheppard and A.P. Davis, *J. Am. Chem. Soc*. 2014, **136**, 12507-12512.
31 M. Boiocchi, L. Del Boca, D. Esteban-Gómez, L. Fabbrizzi, M. Licchelli and E. Monzani, *Chem. Eur. J.* **2005,** *11*, 3097-3104.
32 L.E. Karagiannidis, C.J.E. Haynes, K.J Holder, I.L. Kirby, S.J. Moore, N.J. Wells and P.A. Gale, *Chem. Commun.* 2014, **50**, 12050-12053.
33 S. Altomonte and M. Zanda, *J. Fluorine Chem.* 2012, **143**, 57-93.
34 M.F. Sowaileh, R.A. Hazlitt and D.A. Colby, *ChemMedChem* 2017, **12**, 1481-1490.
35 V. Saggiomo, S. Otto, I. Marques, V. Félix, T. Torroba and R. Quesada, *Chem. Commun.* 2012, **48**, 5274-5276.
36 M.J. Spooner, and P.A. Gale, *Chem. Commun.* 2015, **51**, 4883-4886.
37 N.J. Knight, E. Hernando, C.J.E. Haynes, N. Busschaert, H.J. Clarke, K. Takimoto, M. García-Valverde, J.G. Frey, R. Quesada and P.A. Gale, *Chem. Sci.* 2016, **7**, 1600-1608.
38 N. Busschaert, S.-H. Park, K.-H. Baek, Y.P. Choi, J. Park, E.N.W. Howe, J.R. Hiscock, L.E. Karagiannidis, I. Marques, V. Félix, W. Namkung, J.L. Sessler, P.A. Gale and I. Shin, *Nature Chemistry* 2017, **9**, 667-675.
39 S.-H. Park, S.-H. Park, E.N W. Howe, J.Y. Hyun, L.-J. Chen, I. Hwang, G. Vargas-Zuñiga, N. Busschaert, P.A .Gale, J.L. Sessler and I. Shin, *Chem* 2019, 5, 2079-2098.
40 M. Fares, X. Wu, D. Ramesh, W. Lewis, P.A. Keller, E.N.W. Howe, R. Pérez-Tomás and P.A. Gale, *Angew. Chem. Int. Ed.* 2020, **59**, 17614-17621.

Please do not adjust margins

Please do not adjust margins

41 X. Wu, J.R. Small, A. Cataldo, A.M. Withecombe, P. Turner, P.A. Gale, *Angew. Chem. Int. Ed.* 2019, **58**, 15142-15147.
42 H. Valkenier, O. Akrawi, P. Jurček, K. Sleziaková, T. Lízal, K. Bartik and V. Šindelář, *Chem* 2019, **5**, 429-444.
43 X. Wu, E.N.W. Howe and P.A. Gale, *Acc. Chem. Res*. 2018, **51** , 1870-1879.
44 X. Wu, L.W. Judd, E.N.W. Howe, A.M. Withecombe, V. Soto-Cerrato, H. Li, N. Busschaert, H. Valkenier, R. Pérez-Tomás, D.N. Sheppard, Y.B. Jiang, A.P. Davis and P.A. Gale, *Chem* 2016, **1**, 127-146.
45 X. Wu and P.A. Gale, *Chem. Commun.* 2021, **57**, 3979-3982.
46 Y. Yang, X. Wu, N. Busschaert, H. Furuta, and P.A. Gale, *Chem. Commun.* 2017, **53**, 9230-9233.
47 M. Zarei, M. Vázquez Carrera, S. Vázquez Cruz, R. Leiva MartÍnez, E. Pujol Bech, 2017, *Hri activators useful for the treatment of cardiometabolic diseases*, WO2018010856A1.

Please do not adjust margins